Available online at www.sciencedirect.com
ScienceDirect
Bioorganic & Medicinal Chemistry 14 (2006) 7936–7942
Bioorganic & Medicinal Chemistry

Computational evidence for the ligand selectivity to the α4β2 and α3β4 nicotinic acetylcholine receptors

Hongbin Yuan and Pavel A. Petukhov*

Department of Medicinal Chemistry and Pharmacognosy, College of Pharmacy, University of Illinois at Chicago, 833 S. Wood Street, Chicago, IL 60612, USA

Received 27 May 2006; revised 25 July 2006; accepted 26 July 2006
Available online 21 August 2006

Abstract—The homology models of the α4β2 and α3β4 nicotinic acetylcholine receptors (nAChRs) suggest that the two nAChR subtypes are different in their ligand-binding pockets due to the non-conserved residues in the β-subunits. The docking of nicotine, epibatidine, A-84543, and the two analogs of A-84543 ligands **1** and **2** to the homology models of α4β2 and α3β4 is presented. It is found that the protonated amino groups of these ligands bind to the α-subunits, whereas the remaining parts of the ligands bind to the β-subunits. The two non-conserved amino acids Lys77 and Phe117 in the β2-subunit corresponding to Ile77 and Gln117 in the β4-subunit are identified to be the key players determining the binding modes of the ligands. We demonstrate how the increase in the number of the atoms connecting the pyrrolidine and pyridine rings in A-84543, **1**, and **2**, and an introduction of the alkynyl substituent in the pyridine ring affect the binding and shift the selectivity of these ligands toward the β2-containing receptors. Further improvement in affinity and selectivity in this and other series of the ligands may be achieved by designing molecules that would specifically target the non-conserved regions in nAChRs.

1. Introduction

The nicotinic acetylcholine receptors (nAChRs) are ligand-gated ion channels in the central and peripheral nervous systems.[1,2] These receptors have been identified as promising targets for the treatment of neurological disorders, such as Alzheimer's disease, Parkinson's disease, dyskinesias, Tourette's syndrome, schizophrenia, attention deficit disorder, anxiety, and pain.[3–5] The combinatorial assembly of the 12 neuronal nAChR subunits (α2–α10 and β2–β4) results in homo- or heteropentamers of nAChRs, which consist of the intracellular, transmembrane, and extracellular domains. A ligand-binding site was found at the interface between the two adjacent subunits in the extracellular domain of nAChRs.[6]

A series of pharmacophore models of the nAChR ligands have been proposed and used for the design of novel ligands.[7–12] Generally, these models consist of a quaternary positively charged nitrogen and a hydrogen-bond acceptor at the distance of 4.5–6 Å. The recently solved crystallographic structure of the acetylcholine-binding protein (AChBP),[13,14] in which the residues relevant for the ligand binding are conserved with the nAChR family, provides an opportunity to investigate the ligand–receptor interactions in nAChRs. The homology of the loops forming the binding pocket ranges between 40% and 60% for various nAChR subtypes.[15–17] In recent years, several homology models of the ligand-binding domains have been generated for different neuronal nAChR subtypes; the ligand binding to nAChRs has also been modeled for a limited number of ligands such as nicotine, acetylcholine, and carbamylcholine.[15,17,18] These modeling studies have the consistent results that all the ligands bind at the interface of the two neighboring subunits with the protonated amino group of the ligands docked in the conserved aromatic pocket.

The development of subtype-selective nAChR ligands is a critical issue for an effective and safe treatment of the associated neurodegenerative disorders. As the most abundant subtype of nAChRs in the brain, α4β2 is a major target for neurodegenerative drug development. α3β4 is the most common subtype of nAChRs mediat-

Keywords: Nicotinic acetylcholine receptor; Selectivity; Docking; Non-conserved amino acid.
* Corresponding author. Tel.: +1 312 996 4174; fax: +1 312 996 7107; e-mail: pap4@uic.edu
URL: http://medchem.pharm.uic.edu/

0968-0896/$ - see front matter © 2006 Elsevier Ltd. All rights reserved.
doi:10.1016/j.bmc.2006.07.049

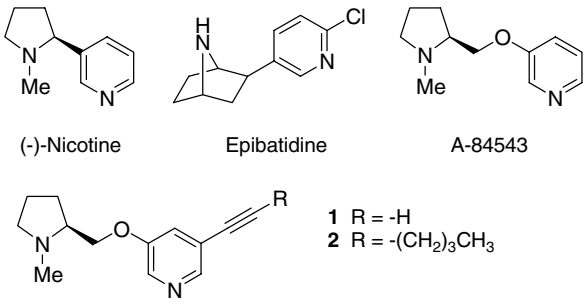

Figure 1.

Table 1. Binding affinities (K_i, nM) of (±)-epibatidine, (−)-nicotine, A-84543, and ligands **1** and **2** to the α3β4 and α4β2 subtypes of nAChRs[19]

Compound	Observed K_i (nM)		
	α3β4	α4β2	α3β4/α4β2
Epibatidine	0.57	0.061	9
Nicotine	443	10	44
A-84543	1400	1.9	737
1	6800	1.6	4250
2	40,000	1.4	28,571

ing the cholinergic events in the autonomic nervous system and therefore the inhibition of the α3β4 subtype is undesirable. It was found that the introduction of an alkynyl group at the C5 position of the pyridyl ring of A-84543, a nicotine analog, results in a dramatic improvement of the ligand selectivity to the β2-containing nAChR subtypes (Fig. 1 and Table 1).[19] The reasons for this improvement were undetermined. In this paper, we present the modeling results of the binding of epibatidine, nicotine, A-84543, and its two analogs to the homology models of the extracelluar domain of α4β2 and α3β4. We show that the non-conserved amino acids of the β subunits in the ligand-binding pockets have significant effects on the binding modes of the ligands and the resulting differences may explain the ligand selectivity to the β2-containing nAChR subtype α4β2.

2. Results and discussion

2.1. The ligand-binding pockets in AChBP, the α3β4 and α4β2 nAChRs

One ligand-binding site exists at each of the five interfaces between the subunits of the pentamer structures of AChBP and the α7 nAChR.[14,20] In the heterologous nAChRs, the ligand binding sites exist only at the interface of two nAChR subunits with an α-subunit on the principal side (α-side) and a β-subunit on the complementary side (β-side).[20] Both of the ligand-binding pockets in AChBP and nAChRs are composed of fairly conserved amino acids (Fig. 2).[13,15–17] The previous modeling studies suggested that the four aromatic amino acids Tyr91, Trp147, Tyr188, Tyr195 and the two adjacent cysteines Cys190 and Cys191 on the α-side are conserved between the α3 and α4 nAChR subunits and AChBP.[15,17,18] Among the residues on the β-side of the binding pocket, Trp55 and Leu119 are conserved between β2 and β4; three non-conserved residues are Lys77, Val109, Phe117 in β2 and Ile77, Ile109, Gln117 in β4. These non-conserved residues in the binding sites are only located on the β-sides of the nAChRs. This is consistent with the biological data suggesting that the differences of the amino acids in the β subunits of nAChRs are responsible for the subtype selectivity of the ligands.[21]

To explore the ligand-binding modes in AChBP, α3β4 and α4β2, we first examined the solvent accessible surface areas at the interfaces of the protein structures close to the ligand binding sites. The 3D structures of the binding pockets on the principal side of AChBP, α3β4, and α4β2 are almost identical (Figs. 3A–C). In each of the three proteins the conserved residues form a narrow hydrophobic pocket. It has been proposed that the cation-π interaction exists between the protonated amino group of the nicotine molecule and the aromatic side chain of Trp147, one of the conserved aromatic amino acids on the α-side.[22–24] On the β-side the ligand-binding pockets of α4β2 and α3β4 have significantly different lipophilic potential, charge distribution, and protein topology patterns. These differences are mainly attributed to the non-conserved residues of the β2 and β4 nAChR subunits (Figs. 3E and F). The area in close proximity to Phe117 in β2 is lipophilic; the same area in β4 is hydrophilic as it is adjacent to Gln117. The area in β2 occupied by Lys77 is hydrophilic and positively charged, whereas in β4 this area is occupied by the shorter lipophilic side chain of Ile77. The areas between Phe117 and Lys77 in β2 and between Gln117 and Ile77 in β4 are occupied by the non-conserved lipophilic residues β2/Val109 and β4/Ile109, respectively.

2.2. Nicotine and epibatidine bound to AChBP, α4β2, and α3β4

We decided to model the ligand binding of nAChRs using the Autodock program in which the binding free-energy function has a desolvation term that calculates the impact of solvent on the ligand binding.[31] To validate the docking results, the nicotine molecule was extracted from the X-ray structure of the nicotine–AChBP complex and re-docked into the AChBP protein. It was found that the Autodock program can successfully reproduce the binding mode of the nicotine molecule in AChBP. The root mean square deviation (rmsd) between the docked and experimental positions of the nicotine molecule is only 0.19 Å, which is substantially less than the resolution of the X-ray structure in the PDB file.

The nicotine and epibatidine molecules were docked to the homology models of the α4β2 and α3β4 nAChR subtypes and the resulting complexes are shown in Figure 4. The docking of nicotine and epibatidine to α4β2 indicates that both compounds form two H-bonds. One hydrogen bond is formed between the protonated amino group and the backbone carbonyl group of α4/Trp147, the other between the pyridyl nitrogen and the backbone NH group of β2/Leu119. The similar pattern of hydro-

```
achbp    -EFDRADILYN---IRQTSRPDVIPTQRDRPVAVSVSLKFINILEVNEITNEVDVVFWQQTTWSDRTLAWNS
alpha3   AEHRLFQYLFED--YNEIIRPVANVSH---PVIIQFEVSMSQLVKVDEVNQIMETNLWLKQIWNDYKLKWKP
alpha4   AEERLLKRLFSG--YNKWSRPVANISD---VVLVRFGLSIAQLIDVDEKNQMMTTNVWVKQEWHDYKLRWDP
beta2    TEERLVEHLLDPSRYNKLIRPATNGSE---LVTVQLMVSLAQLISVHEREQIMTTNVWLTQEWEDYRLTWKP
beta4    AEEKLMDDLLNKTRYNNLIRPATSSSQ---LISIRLELSLSQLISVNEREQIMTTSIWLKQEWTDYRLAWNS
                                                                       55

                             91
achbp    SHSP--DQVSVPISSLWVPDLAAYNAIS-KPEVLTPQLARVVSDGEVLYMPSIRQRFSCDVSGVDTESG-AT
alpha3   SDYQGVEFMRVPAEKIWKPDIVLYNNADGDFQVDDKTKALLKYTGEVTWIPPAIFKSSCKIDVTYFPFDYQN
alpha4   GDYENVTSIRIPSELIWRPDIVLYNNADGDFAVTHLTKAHLFYDGRVQWTPPAIYKSSCSIDVTFFPFDQQN
beta2    EDFDNMKKVRLPSKHIWLPDVVLYNNADGMYEVSFYSNAVVSYDGSIFWLPPAIYKSACKIEVKHFPFDQQN
beta4    SCYEGVNILRIPAKRVWLPDIVLYNNADGTYEVSVYTNVIVRSNGSIQWLPPAIYKSACKIEVKHFPFDQQN
                77                              109       117 119

                147                                        188 190191 195
achbp    CRIKIGSWTHHSREISVDPTTENSDDSEYFSQYSRFEILDVTQKKNSVTYSCCPEAYEDVEVSLNFRKKG
alpha3   CTMKFGSWSYDKAKIDLVLIGS-SMNLKDYWESGEWAIIKAPGYKHEIKYNCCEEIYQDITYSLYIRRLP
alpha4   CTMKFGSWTYDKAKIDLVSMHS-RVDQLDFWESGEWVIVDAVGTYNTRKYECCAEIYPDITYAFIIRRLP
beta2    CTMKFRSWTYDRTEIDLVLKSD-VASLDDFTPSGEWDIIALPGRRNENPDD---STYVDITYDFIIRRKP
beta4    CTLKFRSWTYDHTEIDMVLKSP-TAIMDDFTPSGEWDIVALPGRRTVNPQD---PSYVDVTYDFIIKRKP
```

Figure 2. Sequence alignment between AChBP and N-terminal domains of rat α3, α4, β2, and β4 nAChR subunits. The conserved residues in the binding pockets are labeled and colored red; the non-conserved residues in the binding pockets are labeled and colored blue. The sequence numbers are as the same as the residue numbers in the homology models of the α4β2 and α3β4 nAChRs.

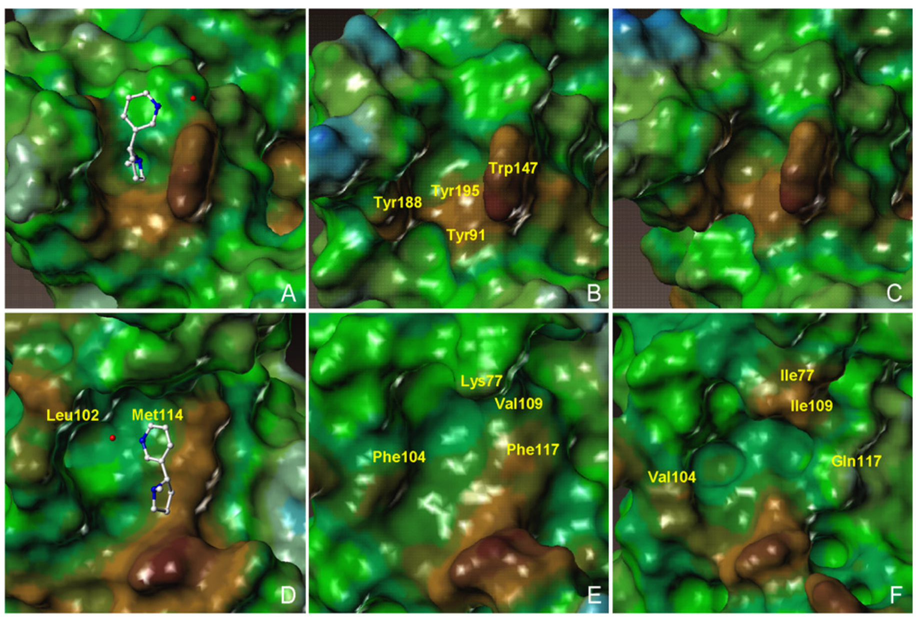

Figure 3. Protein surface of the principal side of the binding pocket mapped by the lipophilic potential: (A) the nicotine–AChBP complex, the water molecule is shown in red, (B) α4 and (C) α3; protein surface of the complementary side of the binding pocket mapped by the lipophilic potential: (D) the nicotine–AChBP complex, (E) β2, (F) β4. The positions of the conserved residues among AChBP, α4 and α3 are shown in B; the positions of the non-conserved residues between β2 and β4 are shown in E and F, respectively. On the protein surface areas, blue stands for hydrophilic, brown for lipophilic, and green for neutral.

gen bonds was observed in the nicotine–AChBP complex where nicotine also forms the hydrogen bonds with Trp143 and the water molecule.[14] The pyridine rings of nicotine and epibatidine are located in close proximity to β2/Phe117, which was proposed to be important for the high affinity of nicotine to the β2-containing receptors.[15] Compared to nicotine, epibatidine is able to bury more of its bulky protonated amino group into the hydrophobic pocket formed by the conserved aromatic amino acids Tyr91, Trp147, Tyr188, Tyr195 and therefore may have stronger cation-π and hydrophobic interactions with the protein. This difference in the binding of nicotine and epibatidine is consistent with the higher affinity of epibatidine to α4β2.

The docking of nicotine and epibatidine to α3β4 shows that the protonated amino groups of both ligands are located in the similar place as in α4β2. Unlike α4β2, in α3β4 neither nicotine nor epibatidine can form a hydrogen bond between the pyridyl nitrogen atom and the backbone NH group of β4/Leu119. Moreover, the β4 subunit cannot stabilize the pyridine ring of the ligands by the π–π or hydrophobic interaction because Gln117 in β4—the counterpart corresponding to Phe117 in β2—cannot form these types of interactions. The loss of these highly favorable interactions may explain the 9- and 44-fold drops in the affinities of epibatidine and nicotine to α3β4, respectively, compared to their affinities to α4β2.

2.3. A-84543 and ligands 1 and 2 bound to α4β2 and α3β4

The increased number of the atoms connecting the pyrrolidine and pyridine rings in A-84543 and its two

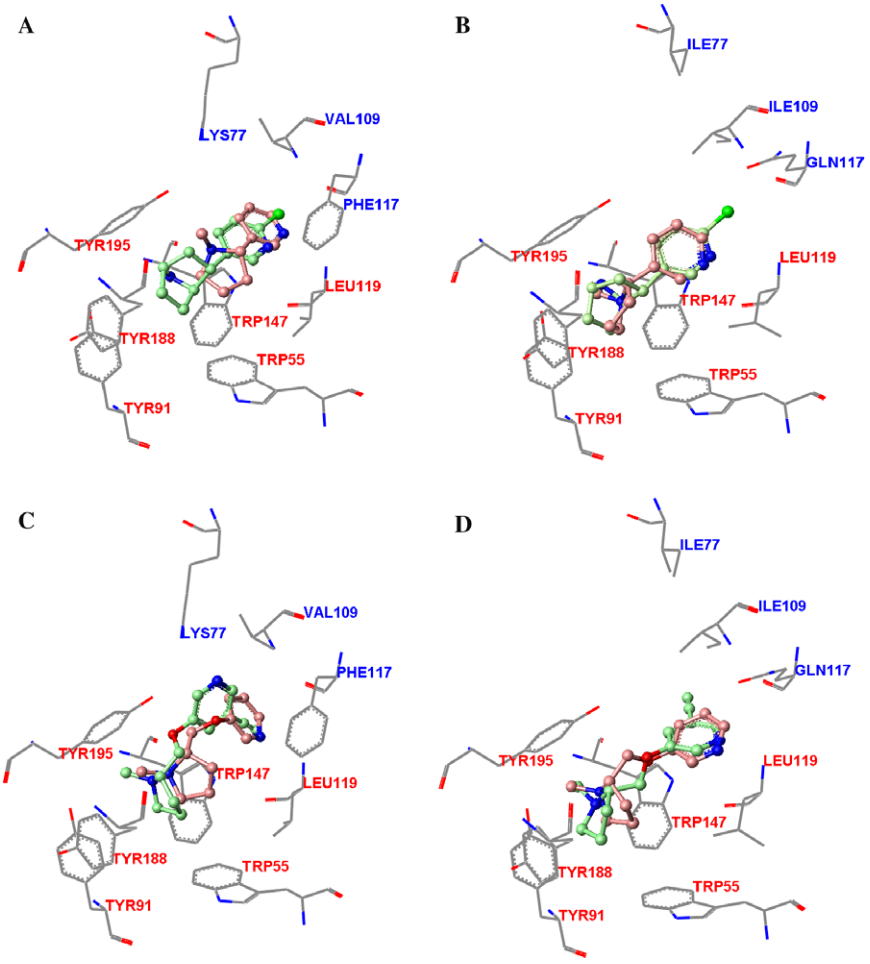

Figure 4. Nicotine and epibatidine bound to (A) α4β2 and (B) α3β4; A-84543 and ligand **1** bound to (C) α4β2 and (D) α3β4. Nicotine and A-84543 are shown in pink; epibatidine and ligand **1** are shown in green. The conserved and non-conserved residues of α4β2 and α3β4 are labeled with red and blue, respectively.

analogs compared to that in nicotine and epibatidine results in different binding modes (Figs. 4 and 5). The pyridyl groups of A-84534 and ligands **1** and **2** bind closer to the non-conserved residues on the β-side of the ligand-binding pocket. This observation may indicate that in general the non-conserved residues play a more important role in the binding of the ligands maintaining a larger distance between the two rings.

Similar to the binding mode of the pyridine rings of nicotine and epibatidine to the ligand-binding pocket of α4β2, the pyridyl nitrogen of A-84543 bound to α4β2 forms a hydrogen bond with the backbone NH of β2/Leu119, whereas the pyridine ring forms the favorable π–π and hydrophobic contacts with β2/Phe117. In α3β4, the pyridyl group of A-84543 facing Gln117 moves away and the pyridyl nitrogen atom cannot form a hydrogen bond with the backbone NH of Leu119. Besides that, A-84543 forms a hydrogen bond with both α4β2 and α3β4 between the protonated pyrrolidine nitrogen atom and the carbonyl group of Trp147.

The docking of ligand **1** shows that its binding modes in α4β2 and α3β4 differ by the position of the pyridine ring and the C5-substituted alkynyl group. In α4β2 the pyridyl nitrogen of **1** has a hydrogen bond with the protonated amino group of the side chain of β2/Lys77 instead of the backbone NH of β2/Leu119, whereas the substituted pyridine ring still maintains the π–π and hydrophobic interactions with the phenyl ring of β2/Phe117. None of these interactions were found for ligand **1** docked to α3β4—the pyridine ring of **1** can neither form a hydrogen bond with the backbone NH of Leu119 nor can it form any favorable interactions with β4/Gln117. The alkynyl group turns to face Ile77 and Ile109 and forms favorable hydrophobic interactions in α3β4. Additionally, the protonated amino group of ligand **1** changes its orientation in the aromatic pocket so that it loses the hydrogen bond with the carbonyl group of Trp147, a favorable interaction found for A-84543 docked to α3β4. Overall, A-84543 and ligand **1** maintain the similar network of interactions with α4β2 and thus have a similar affinity to α4β2, 1.9 and 1.6 nM, respectively. The different binding of A-84543 and ligand **1** to α3β4 is consistent with the fivefold drop in affinity of **1** to α3β4 compared to that of A-84543.

Although ligand **2** has a flexible side chain, Autodock found converged results of the bound conformations of the ligand in α4β2 and α3β4 through the exhaustive

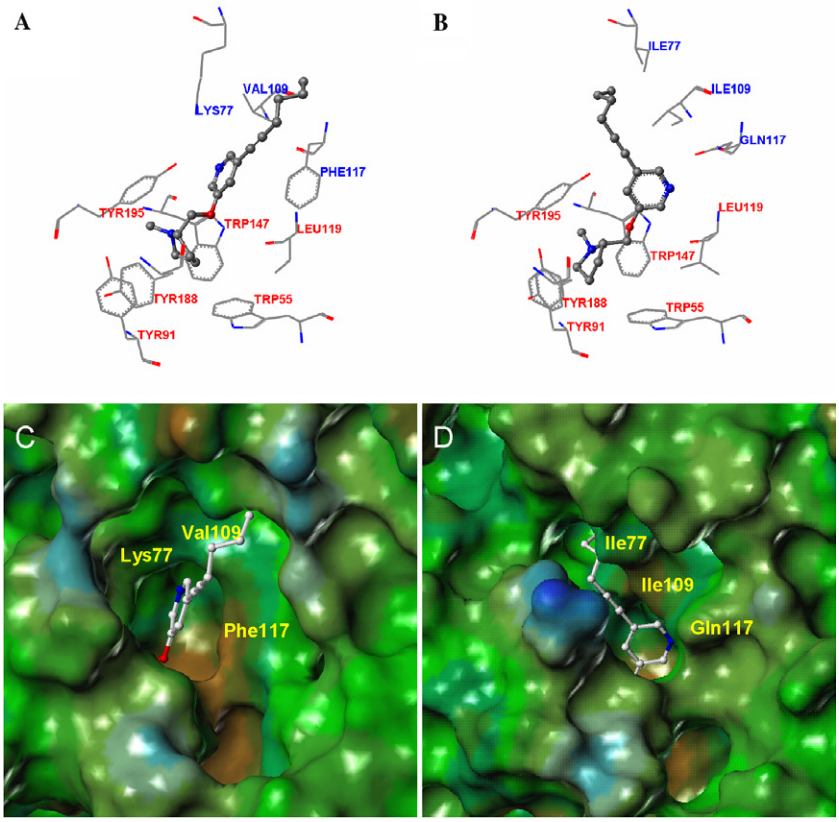

Figure 5. Ligand **2** bound to (A and C) α4β2 and (B and D) α3β4. Ligand **2** is shown in the ball and stick style. The conserved and non-conserved residues in the binding pockets of α4β2 and α3β4 are labeled with red and blue in A and B, respectively. The positions of the non-conserved residues in α4β2 and α3β4 are shown with yellow in C and D. The protein surface is mapped by the lipophilic potential (blue—hydrophilic, brown—lipophilic, and green—neutral).

docking processes. The binding modes of ligand **2** in α4β2 and α3β4 are shown in Figure 5. In α4β2, the pyridine ring of **2** forms the favorable π–π and hydrophobic interactions with the phenyl ring of Phe117, whereas the pyridyl nitrogen forms a hydrogen bond with the side-chain amino group of Lys77. The similar π–π or hydrophobic interaction between the pyridyl ring of **2** and α3β4 is not possible since in β4 the position of the aromatic β2/Phe117 is occupied by the polar Gln117. As the side chain of the non-conserved β4/Ile77 occupies less space than the side chain of the corresponding β2/Lys77, α3β4 contains an additional internal channel in the binding pocket. On the β-side the entrance to this channel is formed by the lipophilic side chains of β4/Ile77 and β4/Ile109. The geometry changes of the protein caused by the non-conserved β4/Ile77 and β4/Gln117 in α3β4 force the long alkynyl substituent of ligand **2** to rotate about 90° compared to its position in α4β2 and to occupy the channel that is unique for the α3β4 subtype. Similar to ligand **1** in α3β4, the protonated amino group of **2** cannot form a hydrogen bond with the backbone carbonyl group of Trp147, a favorable interaction found in the complex between ligand **2** and α4β2. The significant differences in the binding mode of ligand **2** in α3β4 compared to the other ligands and the loss of the majority of the favorable interactions may explain the lowest affinity of **2** to α3β4 among all the ligands studied.

3. Summary

The docking results of nicotine, epibatidine, A-84543, and the two analogs of A-84543 show that the protonated amino groups of all the ligands were predicted to bind within the same region of the binding pockets in α3β4 and α4β2, which is consistent with the experimental data[1] and previous modeling results.[15,17,18] On the other hand, the binding modes of the pyridyl moieties of these ligands may change depending on the length of the linker connecting the two nitrogen atoms. The binding modes of the ligands also change with the introduction of an additional substituent to the pyridine ring. The non-conserved residues β2/Lys77, β2/Phe117 and corresponding β4/Ile77, β4/Gln117 are identified to be the major contributors to the differences in the topology and electrostatic environment of the α4β2 and α3β4 nAChRs. Although the changes caused by these residues are significant, they are relatively remote to the binding of the pyrrolidine and azabicycloheptane rings of the ligands. Therefore, only the ligands with the substituents that are able to reach the areas near β2/Lys77, β2/Phe117 or β4/Ile77, β4/Gln117 and efficiently utilize the differences in the structures of the binding pockets caused by these non-conserved residues would have greater potential to exhibit different levels of affinity and selectivity at the α4β2 and α3β4 nAChRs. Additional biological and modeling studies are underway to

address the selectivity of these ligands for human nAChRs. The present results add to our understanding of the structural differences between α4β2 and α3β4 nAChRs and can be exploited for the design of new leads in the discovery of medications to treat neurodegenerative disorders such as Alzheimer's and Parkinson's diseases.

4. Materials and computational methodology

The structural and biological data of the ligands—epibatidine, nicotine, A-84543 and its two analogs **1** and **2**—were collected from the paper recently published by Kozikowski et al. (Fig. 1 and Table 1).[19] In that paper, the binding affinities (K_i values) of all the ligands were measured with the rat nicotinic receptor subtypes expressed in stably transfected cell lines.[25] The molecular structures of the ligands were built in Sybyl6.9[26] and minimized using the Tripos force field[27] to a convergence criterion of 0.05 kcal/mol Å.

The homology models of the rat α3β4 (PDB entry 1OLJ) and α4β2 (PDB entry 1OLE) nicotinic receptors were built by Le Novere et al.[15] using the model of chick α7-pentamer as a template, whereas the α7-pentamer was created based on the X-ray structure of AChBP.[13,15] The models of α3β4 and α4β2 were used in our studies without changes. The protein solvent accessible areas with lipophilic potential were generated using the MOLCAD module[28,29] in sybyl6.9. The X-ray structure of AChBP and the α4β2 and α3β4 homology models were aligned using the MODELLER/Align3D module in the Accelrys DS Modeling software package.[30] The resulting sequence alignment between AChBP and the extracelluar domains of rat α3, α4, β2, and β4 nAChR subunits is shown in Figure 2.

Epibatidine, nicotine, A-84543, and its two analogs were docked to the models of the α4β2 and α3β4 nACh receptors using the Autodock3.0 software.[31] AutoDock is an automated docking tool designed to predict how small molecules, such as substrates or drug candidates, bind to a receptor of known 3D structure. A free-energy scoring function, comprising terms for dispersion and repulsion, hydrogen bonding, electrostatics, the entropic cost of binding, and solvation, was calibrated with a variety of structurally known protein–ligand complexes. The flexible docking of the ligand structures was done by the genetic algorithm (GA) in search for favorable bound conformations of the ligands in the sites of the target proteins. Although Autodock can successfully reproduce the bound conformations of the modeling ligands, the absolute values of the binding energies for different structures may be inappropriate for comparison due to uncertainty on the comparative modeling process and relatively large standard errors.[31] The partial charges of the ligands and the proteins were calculated using the Gasteiger–Marsili method[32] and the Kollman force field,[33] respectively, the same methods used by Morris et al. to develop the free-energy function for scoring the binding conformations in the Autodock program. A default protocol of docking was applied except the following parameters: number of GA runs was 50; maximum number of energy evaluations was 2.5×10^8. A grid box with a size of $60 \times 60 \times 60$ and a spacing of 0.375 Å between the grid points was employed and placed at the ligand-binding site. The free energy scores for the ligands were calculated using the scoring function implemented in Autodock3.0. The lowest energy ligand–protein complexes were selected for analysis.

Acknowledgment

We thank Dr. Kozikowski for inspiring discussions and critical suggestions.

References and notes

1. Karlin, A. *Nat. Rev. Neurosci.* **2002**, *3*, 102–114.
2. Lester, H. A.; Dibas, M. I.; Dahan, D. S.; Leite, J. F.; Dougherty, D. A. *Trends Neurosci.* **2004**, *27*, 329–336.
3. Lindstrom, J. *Mol. Neurobiol.* **1997**, *15*, 193–222.
4. Paterson, D.; Nordberg, A. *Prog. Neurobiol.* **2000**, *61*, 75–111.
5. Lloyd, G. K.; Williams, M. *J. Pharmacol. Exp. Ther.* **2000**, *292*, 461–467.
6. Sine, S. M. *J. Neurobiol.* **2002**, *53*, 431–446.
7. Beers, W. H.; Reich, E. *Nature* **1970**, *228*, 917–922.
8. Sheridan, R. P.; Nilakantan, R.; Dixon, J. S.; Venkataraghavan, R. *J. Med. Chem.* **1986**, *29*, 899–906.
9. Barlow, R. B.; Johnson, O. *Br. J. Pharmacol.* **1989**, *98*, 799–808.
10. Barreiro, E. J.; Barreiro, G.; Guimaraes, C. R. W.; de Alencastro, R. B. *J. Mol. Struct.—THEOCHEM* **2000**, *532*, 11–22.
11. Tonder, J. E.; Olesen, P. H.; Hansen, J. B.; Begtrup, M.; Pettersson, I. *J. Comput. Aided. Mol. Des.* **2001**, *15*, 247–258.
12. Wei, Z. L.; Petukhov, P. A.; Xiao, Y.; Tuckmantel, W.; George, C.; Kellar, K. J.; Kozikowski, A. P. *J. Med. Chem.* **2003**, *46*, 921–924.
13. Brejc, K.; van Dijk, W. J.; Klaassen, R. V.; Schuurmans, M.; van Der Oost, J.; Smit, A. B.; Sixma, T. K. *Nature* **2001**, *411*, 269–276.
14. Celie, P. H.; van Rossum-Fikkert, S. E.; van Dijk, W. J.; Brejc, K.; Smit, A. B.; Sixma, T. K. *Neuron* **2004**, *41*, 907–914.
15. Le Novere, N.; Grutter, T.; Changeux, J. P. *Proc. Natl. Acad. Sci. U.S.A.* **2002**, *99*, 3210–3215.
16. Sine, S. M.; Wang, H. L.; Bren, N. *J. Biol. Chem.* **2002**, *277*, 29210–29223.
17. Schapira, M.; Abagyan, R.; Totrov, M. *BMC Struct. Biol.* **2002**, *2*, 1.
18. Costa, V.; Nistri, A.; Cavalli, A.; Carloni, P. *Br. J. Pharmacol.* **2003**, *140*, 921–931.
19. Wei, Z. L.; Xiao, Y.; Yuan, H.; Baydyuk, M.; Petukhov, P. A.; Musachio, J. L.; Kellar, K. J.; Kozikowski, A. P. *J. Med. Chem.* **2005**, *48*, 1721–1724.
20. Corringer, P. J.; Le Novere, N.; Changeux, J. P. *Annu. Rev. Pharmacol. Toxicol.* **2000**, *40*, 431–458.
21. Figl, A.; Cohen, B. N.; Quick, M. W.; Davidson, N.; Lester, H. A. *FEBS Lett.* **1992**, *308*, 245–248.
22. Zhong, W.; Gallivan, J. P.; Zhang, Y.; Li, L.; Lester, H. A.; Dougherty, D. A. *Proc. Natl. Acad. Sci. U.S.A.* **1998**, *95*, 12088–12093.

23. Li, L.; Zhong, W.; Zacharias, N.; Gibbs, C.; Lester, H. A.; Dougherty, D. A. *Chem. Biol.* **2001**, *8*, 47–58.
24. Beene, D. L.; Brandt, G. S.; Zhong, W.; Zacharias, N. M.; Lester, H. A.; Dougherty, D. A. *Biochemistry* **2002**, *41*, 10262–10269.
25. Xiao, Y.; Meyer, E. L.; Thompson, J. M.; Surin, A.; Wroblewski, J.; Kellar, K. J. *Mol. Pharmacol.* **1998**, *54*, 322–333.
26. SYBYL (Version 7.0), Tripos, Inc., 1699 South Hanley Road, St. Louis, MO 63144.
27. Clark, M.; Cramer, R. D.; Vanopdenbosch, N. *J. Comput. Chem.* **1989**, *10*, 982–1012.
28. Ghose, A. K.; Viswanadhan, V. N.; Wendoloski, J. J. *J. Phys. Chem. A* **1998**, *102*, 3762–3772.
29. Viswanadhan, V. N.; Ghose, A. K.; Revankar, G. R.; Robins, R. K. *J. Chem. Inf. Comput. Sci.* **1989**, *29*, 163–172.
30. DS Modeling 1.1, Accelrys Inc., 10188 Telesis Court, Suite 100, San Diego, CA 92121.
31. Morris, G. M.; Goodsell, D. S.; Halliday, R. S.; Huey, R.; Hart, W. E.; Belew, R. K.; Olson, A. J. *J. Comput. Chem.* **1998**, *19*, 1639–1662.
32. Gasteiger, J.; Marsili, M. *Tetrahedron* **1980**, *36*, 3219–3228.
33. Cornell, W. D.; Cieplak, P.; Bayly, C. I.; Gould, I. R.; Merz, K. M.; Ferguson, D. M.; Spellmeyer, D. C.; Fox, T.; Caldwell, J. W.; Kollman, P. A. *J. Am. Chem. Soc.* **1995**, *117*, 5179–5197.